Hydrogen intercalation of epitaxial graphene and buffer layer probed by mid-infrared absorption and Raman spectroscopy

Cite as: AIP Advances **8**, 045015 (2018); https://doi.org/10.1063/1.5024132
Submitted: 30 January 2018 • Accepted: 04 April 2018 • Published Online: 16 April 2018

J. Kunc, M. Rejhon and P. Hlídek

AIP ADVANCES **8**, 045015 (2018)

Hydrogen intercalation of epitaxial graphene and buffer layer probed by mid-infrared absorption and Raman spectroscopy

J. Kunc,[a] M. Rejhon, and P. Hlídek
Institute of Physics, Charles University, Faculty of Mathematics and Physics, Ke Karlovu 5, Prague 2 CZ-121 16, Czech Republic

(Received 30 January 2018; accepted 4 April 2018; published online 16 April 2018)

We have measured optical absorption in mid-infrared spectral range on hydrogen intercalated single layer epitaxial graphene and buffer layer grown on silicon face of SiC. We have used attenuated total reflection geometry to enhance absorption related to the surface and SiC/graphene interface. The Raman spectroscopy is used to show presence of buffer layer and single layer graphene prior to intercalation. We also present Raman spectra of quasi free standing monolayer and bilayer graphene after hydrogen intercalation at temperatures between 790 and 1510°C. We have found that although the Si-H bonds form at as low temperatures as 790°C, the well developed bond order has been reached only for samples intercalated at temperatures exceeding 1000°C. We also study temporal stability of hydrogen intercalated samples stored in ambient air. The optical spectroscopy shows on a formation of silyl and silylene groups on the SiC/graphene interface due to the residual atomic hydrogen left from the intercalation process. https://doi.org/10.1063/1.5024132

I. INTRODUCTION

Graphene as a semi-metal with tunable Fermi level is an alternative concept to modify Schottky or tunneling barriers formed at the graphene/semiconductor or graphene/oxide/metal interface. The top gated epitaxial graphene grown on SiC(000$\bar{1}$)[1] and SiC(0001)[2–4] has been demonstrated. A back-gated epitaxial graphene provides direct access to the graphene/semiconductor interface[5,6] and it would facilitate optical studies without complications caused by underlying substrate.[7] Bottom-gated epitaxial graphene can be also used to reduce carrier scattering caused by top-gate,[8] or it can be used in tunable single molecule transistors.[9] However, backgating of epitaxial graphene grown on silicon face of SiC(0001) has been demonstrated only on hydrogen intercalated graphene.[5,6]

The as—grown epitaxial graphene on SiC(0001) consist of so called zero graphene layer, also called buffer layer, and the single layer graphene (SLG). The buffer layer is known to contain roughly 30%[10] of sp^3 bonded carbon. These carbon atoms are bonded to Si in SiC beneath the buffer layer. Due to the low degree of order of these sp^3 bonds, originating from $6\sqrt{3} \times 6\sqrt{3}R30°$ SiC surface reconstruction, the band structure of buffer contains large amount of localized states.[11] These interface localized states pin the Fermi level when as—grown epitaxial graphene is gated. Another issue is that the buffer layer mediates interaction between carriers in the graphene layer and phonons in SiC, thus significantly reducing carrier mobility in graphene.[12–14] Therefore, the high mobility graphene with tunable Fermi level requires eliminating buffer[15] and thus reducing interaction between graphene and SiC.[16,17] This can be readily done by intercalation of the SiC/buffer interface by molecular[16] or atomic[18,19] hydrogen. Hydrogen saturates Si-C bonds, turns sp^3 carbon back into sp^2 bonded carbon and, as a result, so called buffer-free quasi free standing monolayer graphene (QFSMLG) is formed

[a]Electronic mail: kunc@karlov.mff.cuni.cz

from buffer layer and quasi free standing bilayer graphene (QFSBLG)[16,20] is formed from SLG. The QFSMLG is purely physisorbed on top of SiC substrate.[21] It also exhibits very low buckling and homogeneous electron density at the interface.[21]

Beside hydrogen, also annealing in oxygen,[22] rapid cooling[23] or ion implantation[24] have been shown to turn buffer layer into QFSMLG. However, oxygen annealing and ion implantation can lead to defect formation in graphene and rapid cooling is not suitable for fabrication of electronic devices on large scales. The best solution still seems to be hydrogen intercalation since it is process readily available in semiconductor industry. Hydrogen can be also used to prepare atomically flat SiC surface by hydrogen etching[25] or pit-free surfaces by selective silicon etching at reduced growth temperatures.[26]

The main objective of this work is to study Si-H bond formation and its temporal stability. This will provide a route towards reliable, back-gated epitaxial graphene of high carrier mobility. Although temperature of Si-H bond formation is well known (710°C), it is not clear how this temperature changes in the case of SiC/buffer interface and how well-ordered the Si-H bonds are. In the case of SiC/buffer and SiC/SLG interface, hydrogen has to either tunnel through the single layer graphene and buffer layer, or, it gets in the SiC/buffer interface via defects in graphene and/or buffer. Therefore we assume that the temperature of fully decoupled buffer from SiC is rised at fixed hydrogen intercalation times. The temporal stability of intercalated hydrogen is also investigated here and we discuss potential issues caused by residual atomic hydrogen in the SiC/graphene interface.

II. EXPERIMENTAL RESULTS

The 4*H*-SiC wafers were bought from II-VI Inc. We use on-axis (±0.6°) semi-insulating SiC, 500 μm thick wafers with resistivity $\rho > 10^9$ Ωcm. The conducting nitrogen doped SiC wafers have

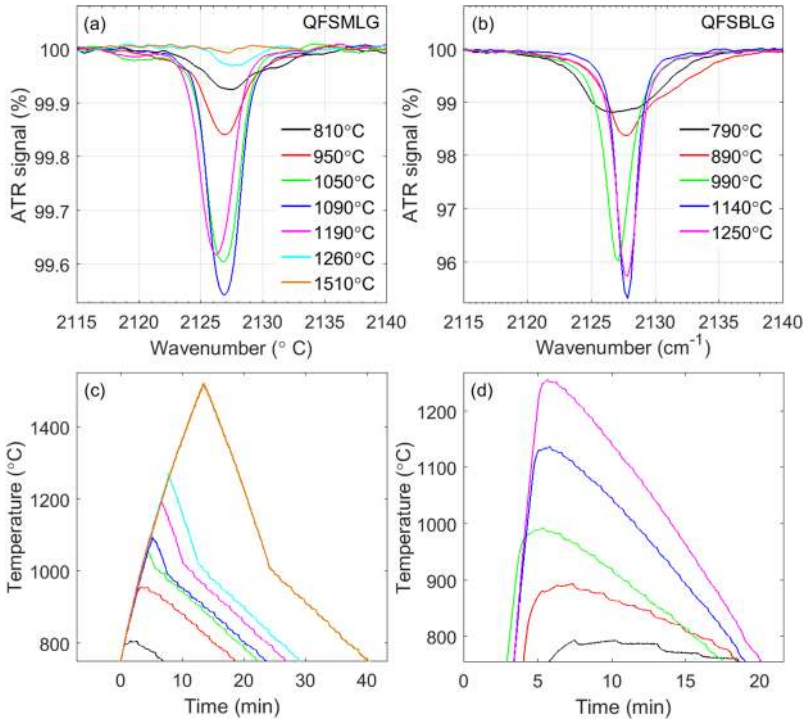

FIG. 1. The ATR spectra of H_2 intercalated (a) buffer layer and (b) single layer graphene on SiC(0001). The growth regimes for H_2 treated (c) buffer layer and (d) single layer graphene. The ATR spectra in (a) and hydrogen intercalation recipes in (b) of buffer layer samples annealed at 810, 950, 1050, 1090, 1190, 1260 and 1510°C are depicted by black, red, green, blue, magenta, cyan and orange curves, respectively. The ATR spectra in (b) and hydrogen intercalation recipes in (d) of single layer graphene samples annealed at 790, 890, 990, 1140 and 1250°C are depicted by black, red, green, blue and magenta curves, respectively.

resistivity $\rho = 15 - 28 \times 10^{-3}$ Ωcm, thickness 350 μm and they are cut 4° off the c-axis (0001). We grow epitaxial graphene on epi-ready (chemically mechanically polished) Si-face. The wafers are diced on 3.5×3.5 mm^2 samples. The single layer epitaxial graphene is grown in inductively heated furnace[27] at 1600-1670°C for 5 minutes in argon atmosphere and argon flow 30 standard liters per hour (SLPH) at 1000 mbar. The buffer layer is grown in the same furnace at 1530-1570°C for 5 minutes at flow of 30 SLPH of purified argon at 1000 mbar. We use the same graphite crucible for the growth of buffer and SLG. More details about the growth conditions can be found in our previous work.[28] Annealing in hydrogen is performed in the range of temperatures from 790° to 1650°C. The hydrogen pressure and flow rate are kept at 1000 mbar and 10 SLPH, respectively. The graphite crucible for hydrogen intercalation is 40 mm long isostatically pressed graphite cylinder with 10 mm diameter. The hole (diameter 5 mm) is drilled from one side so as hydrogen can flow to the sample without any obstacles. Two holes with diameter 2 mm are drilled from the opposite side of the graphite crucible to ensure proper gas flow above the samples. The epitaxial graphene samples are characterized by micro-Raman confocal microscope WITec alpha300 RSA (WITec, Germany) with 532 nm laser excitation (power < 20 mW) in the backscattering geometry with the objective (Zeiss, Germany) of numerical aperture NA=0.9 and 100× magnification. As Si-H bond is formed only at the SiC/graphene interface, the measurements in transmission geometry are precluded by high background signal from bulk SiC. Therefore it is essential to measure by means of Attenuated Total Reflection (ATR),[29] employing evanescent wave of totally reflected light which probes only the SiC surface layer. The probed surface layer thickness is few micrometers, still four orders of magnitude more than the thickness of Si-H layer. The ATR spectra are measured by evacuated Fourier Transform Infrared (FTIR) spectrometer Bruker Vertex80v. The ATR module from Pike Technologies is equipped with a single-reflection germanium crystal. The angle of incidence

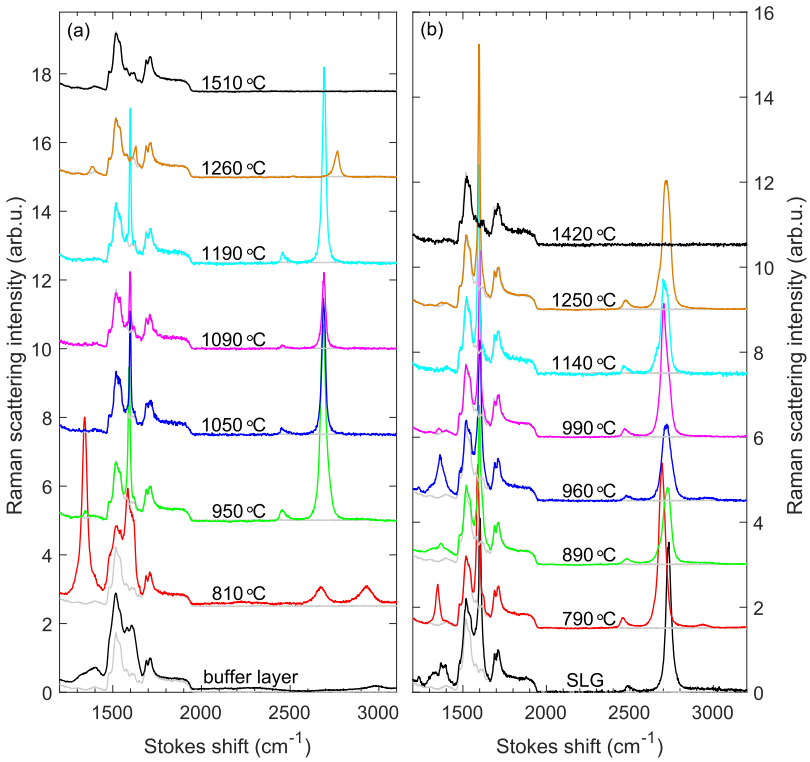

FIG. 2. Raman spectra of hydrogen intercalated (a) buffer layer and (b) single layer epitaxial graphene. The reference spectra of as-grown buffer and as-grown single layer graphene before intercalation are shown by black curves. The Raman spectra as a function of temperature of hydrogen intercalation are depicted and labeled by corresponding maximal intercalation temperature. The spectra are shifted vertically for clarity. Each spectrum is plotted together with a Raman spectrum of bare SiC (grey curves).

is 45°. The sample is placed on top of the crystal and pressed by calibrated pressure clamp. We use a room temperature Deuterated Lanthanum α-Alanine doped TriGlycine Sulphate (DLaTGS) detector.

We compare ATR spectra of H_2 annealed buffer layer, Fig. 1(a) and SLG, Fig. 1(b). The annealing temperature during H_2 intercalation is depicted in Figs. 1(c) and 1(d) for hydrogen intercalation of buffer and SLG, respectively. A well pronounced Si-H absorption band is developed at 2126-2128 cm^{-1}. The maximal absorption is 4.5×10^{-3} in QFSMLG and it is 10× stronger (4.5×10^{-2}) in QFSBLG, see Figs. 1(a) and 1(b). We observe narrowing of the absorption band with increasing temperature of intercalation. The absorption band also exhibits maximum at ≈ 1090°C and at ≈ 1140°C in QFSMLG and QFSBLG, respectively. We have performed Raman spectroscopy to reveal mechanism responsible for observed trends in Si-H absorption band.

The Raman spectra of QFSMLG formed at intercalation temperatures from 810°C to 1510°C are shown in Fig. 2(a). The spectra are compared with the buffer layer Raman spectrum prior to intercalation (black curve in Fig. 1(a)). Hydrogen intercalation of buffer layer results in appearance of G, 2D and D peak, see also detail of 2D peak spectral range prior to intercalation in Fig. 3(c). The 2D peak of intercalated buffer at 1090°C has a Lorentzian line shape with Full Width at Half Maximum (FWHM) 23 cm^{-1} and 2D peak position $\omega_{2D,QFSMLG}$ = 2691.8 cm^{-1}, see Fig. 3(d). The residua between experimental data and fitted Lorenzian curve show $\chi^2 = 2.9$ which belongs to χ^2 statistics with one degree of freedom, as expected for a good fit. We have also calculated second derivative $d^2I/d\omega^2$ of Raman scattering intensity I with respect to Stokes shift ω, see inset of Fig. 3(d). The observed single minimum in $d^2I/d\omega^2$ is a signature of single component 2D peak. The appearance of D, G and 2D, single component Lorenzian line shape of 2D peak and FWHM = 23 cm^{-1} of 2D peak provide evidence of QFSMLG formation. The low temperature intercalation at 810°C leads to

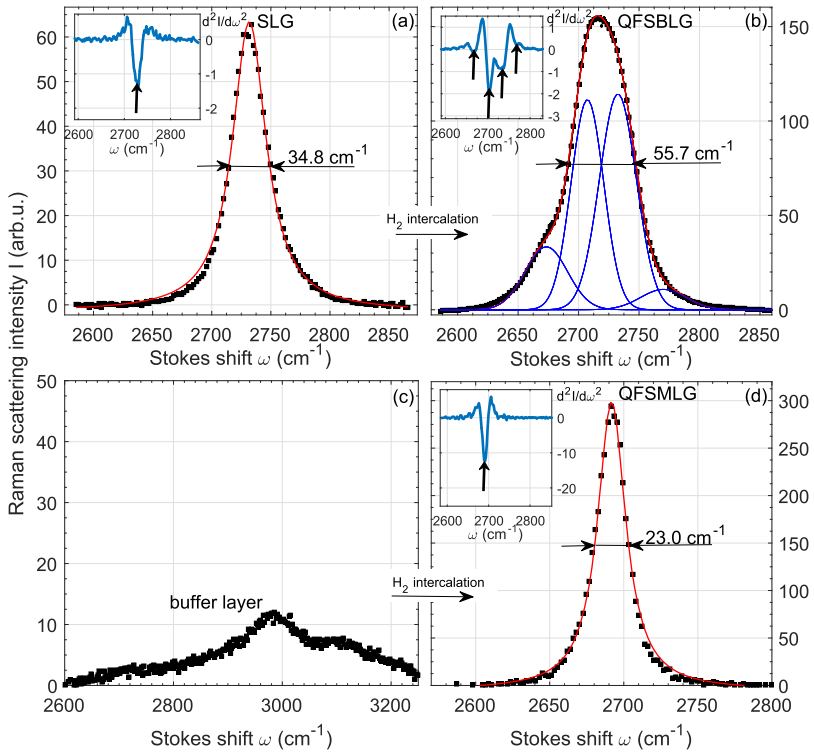

FIG. 3. A 2D peak line shape of (a) SLG, (b) QFSBLG intercalated at 1250°C, (c) buffer layer and (d) QFSMLG intercalted at 1190°C. The black dots are experimental data and red curves are fits by a single Lorentzian peak in the case of (a) SLG and (d) QFSMLG. The 2D peak of (b) QFSBLG was fitted by a sum of four Gaussian peaks. The insets are second derivatives of Raman scattering intensity I with respect to Stokes shift ω. The positions of spectral components of 2D peak determined from minima of $\frac{d^2I}{d\omega^2}$ are marked by arrows in the insets (a, b, d). The four components of 2D peak in QFSBLG are depicted by blue Gaussian peaks in (b).

homogeneous, however incomplete intercalation, Fig. 2(a), red spectrum (810°C). Raman spectrum consists of a mixture of buffer layer and poor quality intercalated graphene. The strong D peak is a fingerprint of small graphene grain size L. The ratio of D peak integrated intensity I_D to G peak integrated intensity I_G is related to the graphene grain size by $L(\text{nm}) = 19\ \text{nm} \times \frac{I_G}{I_D}$ [30–32] when Raman scattering is excited by light at the wavelength 532 nm. We estimate the grain size of about $L \approx 20$ nm for the buffer layer intercalated at 810°C. We also plot each spectrum together with a reference spectrum of bare SiC to better distinguish strength of D peak at higher intercalation temperatures, where the D peak intensity is too low to be distinguished easily from the Raman spectrum of SiC substrate. When Raman spectra of QFSMLG and bare SiC are compared then the D peak can be observed at all intercalation temperatures. There are locally grains with no observable D peak in the samples intercalated at temperatures between 1000-1200°C. The QFSMLG grain size is shown as a function of temperature in Fig. 4(a) by blue squares. The maximal grain size is reached at ≈ 1000 −1100°C. The G peak intensity is reduced at high temperatures above 1200°C due to the hydrogen etching of graphene. The graphene layer is entirely etched away at temperatures as high as 1510°C. We also note that there is no signature of buffer layer in QFSMLG Raman spectra for T > 1000°C, which is commonly observed in SLG. Next, the hydrogen intercalation of SLG is discussed. The Raman spectrum of SLG prior to intercalation, Fig. 2(b) black spectrum, shows ratio of 2D peak

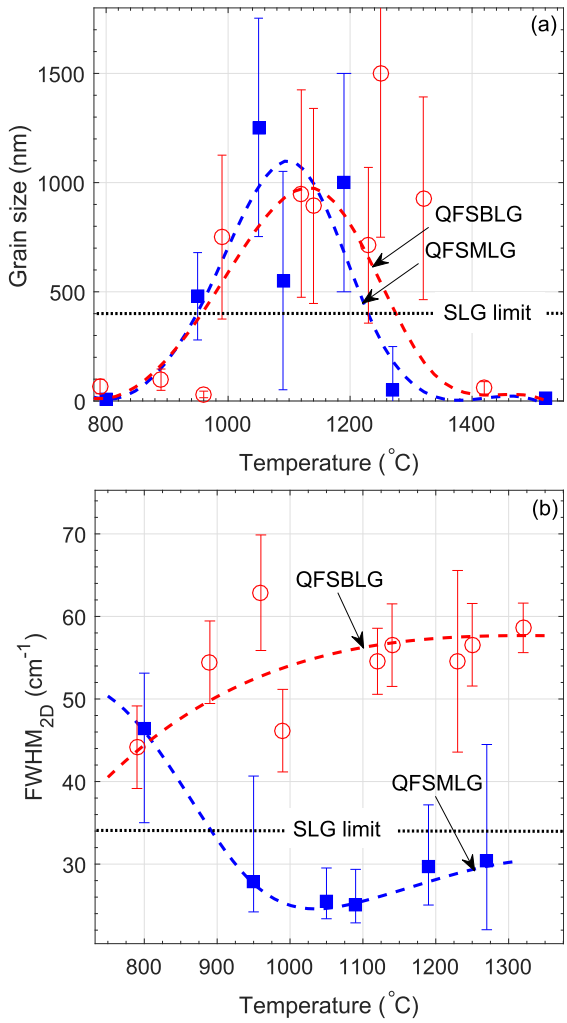

FIG. 4. The (a) grain size and (b) 2D peak FWHM of (blue squares) quasi free standing monolayer graphene and (red circles) quasi free standing bilayer graphene as a function of maximal temperature of hydrogen intercalation. The limits typically reached in SLG are shown by dotted horizontal lines. The dashed lines are guides for eye.

integrated intensity I_{2D} to G peak integrated intensity I_G, I_{2D}/I_G=2.7 (after subtraction of buffer layer signal). The FWHM of 2D peak is 34.8 cm^{-1}. The 2D peak is a single component Lorentzian peak as we show in Fig. 3(a) by a single Lorentzian fit (red curve, χ^2=1.1). The single component 2D peak is also revealed as a single minimum of $d^2I/d\omega^2$, see inset in Fig. 3(a). These are fingerprint characteristics of SLG. The hydrogen intercalation of SLG at 1250°C turns a single component Lorentzian 2D peak ($\omega_{2D,SLG}$ = 2731.8 cm^{-1}) into a four component 2D peak, as shown by a four component Gaussian fit in Fig. 3(b) (χ^2 = 1.17) and by four minima in $d^2I/d\omega^2$, see inset in Fig. 3(b). The FWHM of 2D peak is 55.7 cm^{-1}. The spectral positions of these four components are 2673.3, 2707.3, 2732.5 and 2770.1 cm^{-1} and their FWHMs are 41.3, 31.7, 36.0 and 44.2 cm^{-1}, respectively. The four component 2D peak and its broadening evolved from a SLG provide experimental evidence of QFSBLG. The Raman spectra of QFSBLG formed at temperatures from 790°C to 1420°C are shown in Fig. 2(b). The formation of strong D peak at low temperatures below 990°C is again, similarly to QFSMLG, a signature of incomplete intercalation. The QFSBLG with low D peak intensity is formed at temperatures $T \geq 990°C$. The largest grain size of QFSBLG is reached in the range of intercalation temperatures 1000-1250°C, shown in Fig. 4(a) by red circles.

The FWHM of 2D peak is another parameter related to the graphene quality.[33] The temperature dependence of the FWHM is shown in Fig. 4(b) for QFSMLG (QFSBLG) by blue squares (red circles). The minimal FWHM of (25±3) cm^{-1} is reached at 1050-1090°C in QFSMLG. The low mean FWHM of 25 cm^{-1} together with a low standard deviation $\sigma_{FWHM,2D}$ = 3 cm^{-1} is a fingerprint of high carrier mobility.[33] The FWHM of 2D peak in QFSBLG has a monotonously increasing character from 44 cm^{-1} at T = 790°C to 57 cm^{-1} at 1330°C. This gradually increasing FWHM can be explained by gradually increasing degree of transition from SLG (FWHM 34 cm^{-1}) to well developed QFSBLG (FWHM 57 cm^{-1}).

In the following paragraph we correlate observed evolution of Raman spectra with integrated intensity and FWHM of Si-H absorption band measured by ATR mid-infrared spectroscopy. The H_2 intercalation at temperatures as low as 790-810°C leads to relatively weak (Figs. 5(b) and 5(d))

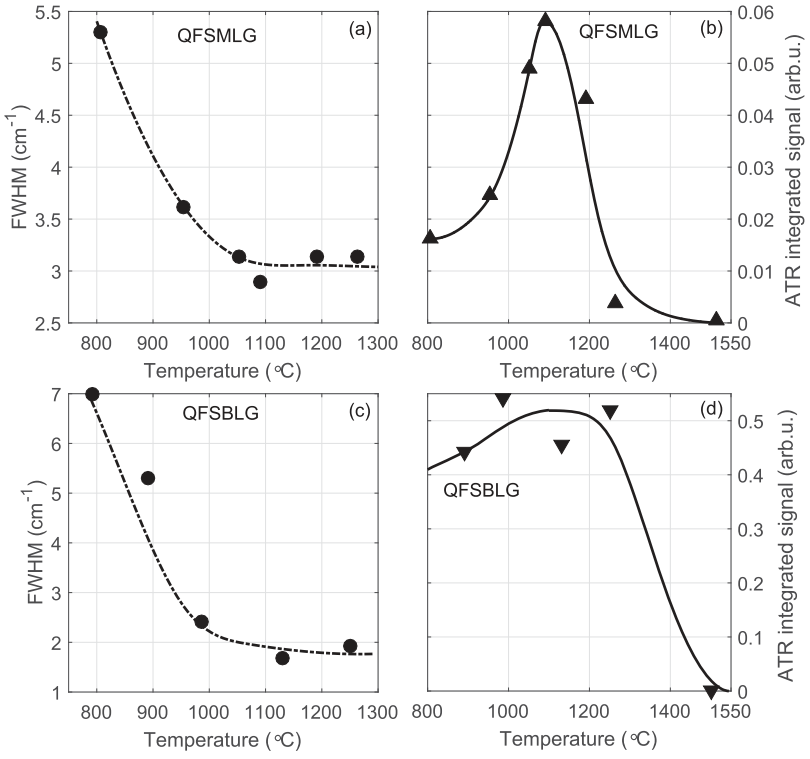

FIG. 5. (a, c) The Full Width at Half Maximum and (b, d) integrated ATR signal of Si-H absorption band for (a, b) quasi free standing monolayer graphene (QFSMLG) (intercalated buffer layer) and (c, d) quasi free standing bilayer graphene (QFSBLG) (intercalated SLG).

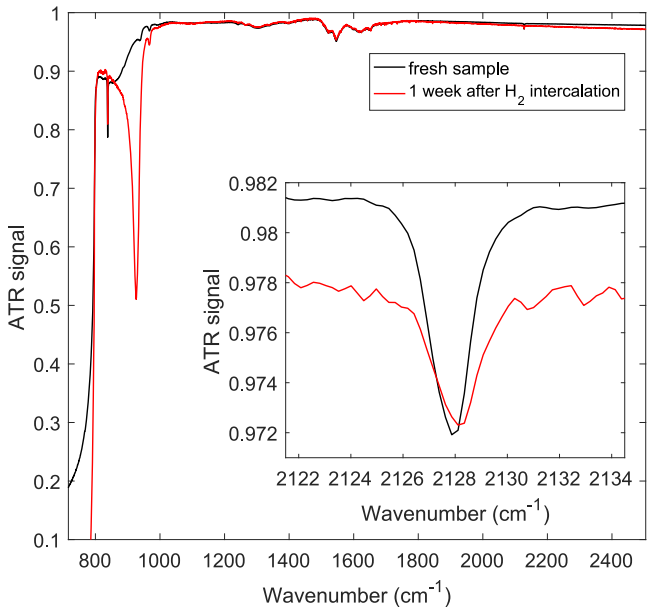

FIG. 6. ATR spectra of single layer graphene sample measured (black curve) immediately after H_2 intercalation and (red curve) one week after the annealing. The sample was stored in air. (inset) Detail of Si-H absorption band as measured (black curve) immediately after H_2 intercalation and (red curve) one week after the annealing.

and broad (Figs. 5(a) and 5(c)) Si-H absorption band. As the temperature is rised the FWHM of the Si-H band narrows and the FWHM saturates at $\delta\omega = (3.0 \pm 0.2)$ cm^{-1} for QFSMLG and at $\delta\omega = (1.8 \pm 0.2)$ cm^{-1} for QFSBLG. We note that the ATR spectra are measured with FTIR spectrometer at the spectral resolution 0.5 cm^{-1}, hence the saturation value $\delta\omega$ is not caused by the minimal spectral resolution of the FTIR spectrometer. The integrated intensity of the Si-H absorption band exhibits sharp maximum at 1090°C in QFSMLG and relatively broader maximum at 1000-1250°C in QFSBLG. These trends in integrated intensity of Si-H absorption band correlate with trends

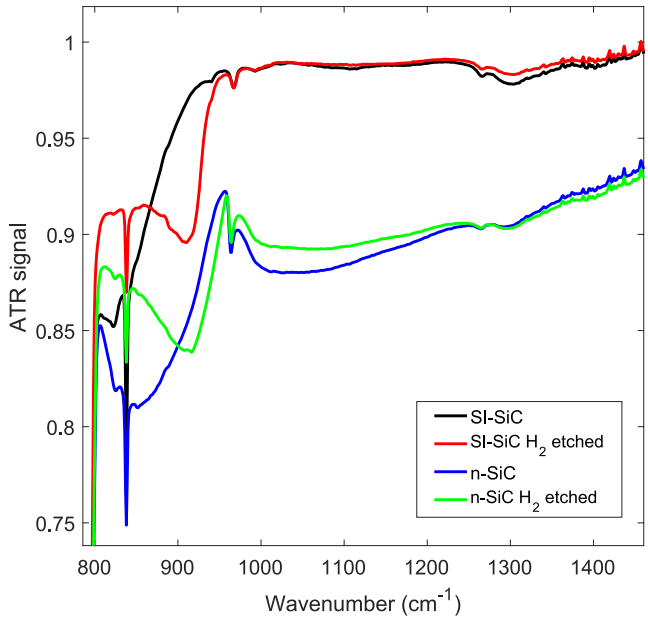

FIG. 7. ATR spectra of SiC (black and blue curves) before H_2 annealing and (red and green curves) after H_2 annealing. The black and red (blue and green) curves correspond to semi-insulating (conducting) SiC.

observed in graphene grain size determined from Raman scattering. The observed narrowing of Si-H absorption band, Fig. 5(a) corresponds to the narrowing of 2D peak in QFSMLG. The narrowing of Si-H absorption band in QFSBLG 5 (c) correlates with saturating FWHM of 2D peak at ≈ 58 cm^{-1}.

We study also temporal stability of H_2 intercalation of SLG. The Si-H bond is well pronounced in the QFSBLG sample measured immediately after H_2 intercalation, as shown by black curve in the inset of Fig. 6. When sample is left in ambient air for one week, the intensity of Si-H absorption band decreases by 50% and its FWHM increases by 4%, as shown by red curve in the inset of Fig. 6. This is evidence of gradually reduced amount of Si-H bonds. The second effect of aging is a newly developed band at 900-940 cm^{-1}. This band can be also formed without aging, as we show in Fig. 7. The band at 900-940 cm^{-1} is formed in bare SiC when we etch the sample at 1650°C for 30 minutes. We observe similar behavior for both semi-insulating and conducting bare SiC samples, as we show in Fig. 7. We note that this band is not observed when annealing temperature of SiC is below 1200 °C.

III. DISCUSSION

We have shown presence of Si-H chemical bonds in hydrogen intercalated buffer layer and SLG. The H_2 intercalation leads to quasi-free standing monolayer and bilayer graphene as has been discussed in literature and confirmed by our Raman spectroscopy. The bond order can be deduced from the FWHM of 2128 cm^{-1} Si-H absorption band. The observed broadening of this band can be interpreted as lower degree of bond order with respect to the direction perpendicular to the sample surface. The lowest temperature of Si-H bond formation at T_{min} = 700°C corresponds to the onset of Si-H absorption band is SLG samples at $T_{min,SLG}$ = 790°C. This low temperature Si-H bond formation is however not complete as shown by FWHM as large as 7 cm^{-1} and strong D peak in Raman spectra. The well ordered Si-H bonds develop at temperatures 300°C higher (above 1000°C). We interpret this temperature rise as a consequence of additional barrier which hydrogen has to overcome to get in SiC/buffer layer interface. The two possible routes are defects in graphene and buffer, or, since hydrogen is small molecule, it can penetrate through the graphene layer.

We note that our results are not in contradiction with procedures of hydrogen desorption described in literature.[16,19] Hydrogen desorption from QFSMLG and QFSBLG has been reported to occur at about 700°C in vacuum.[19] We confirm by our experiments that hydrogenated samples heated to ≈ 900°C in high vacuum (10^{-5} mbar) for 30 minutes can be recovered nearly to the state before intercalation. However, in contrast do hydrogen desorption, we anneal buffer layer and SLG at 1000 mbar of hydrogen. Our reason for hydrogen intercalation at temperatures well above 700°C is to facilitate transport of hydrogen below buffer layer. The kinetic energy of hydrogen molecules is higher at elevated temperatures. The higher kinetic energy allows faster transport of hydrogen over energetic barriers from the gas phase above sample to the interface between buffer layer and SiC substrate. However, as the Si-H bond does not form at temperatures above 700°C we slowly cool down to ≈ 600°C (10°C/min in our recipes) to allow formation of Si-H bonds when crossing the critical temperature.

Beside the successful H_2 incorporation in the SiC/buffer and SiC/SLG interface, it is also important that the formed intercalated SLG is stable for reliable device operation. Beside our observation that amount of Si-H bonds is reduced by 50% in one week, we have also observed formation of new absorption band at 890-940 cm^{-1}. As we are able also to form this band by annealing SiC(0001) at high temperature (1650°C) for 30 minutes, we argue that it should be related to SiH_x groups formed on the SiC surface. As the FWHM of this absorption band reaches 50 cm^{-1}, it is probably composed of many different types of bonds and configurations. We suggest that energetically these chemical groups could be a silylene radical SiH_2 (900-930 cm^{-1}),[34] deformation mode of a silyl group SiH_3 (920, 843.5, 939.6, 941 cm^{-1}),[35] Si-H bending (937 cm^{-1})[36] or Si-H_2 scissor mode (910 cm^{-1}).[37]

The time evolution of infrared absorption suggests that hydrogen tends to further react with silicon in the buffer/SLG interface layer. This is probably atomic hydrogen left below the buffer layer from the hydrogen intercalation. The observed absorption at 890-940 cm^{-1} can be understood as a step towards gaseous silane, as has been shown experimentally by mass spectrometry where atomic hydrogen reacts with SiC even at room temperature.[38] We note that although we intercalate SLG and

buffer layer by molecular hydrogen, the hydrogen molecule is dissociated prior to bonding to silicon in the process of buffer decoupling. Inevitably, the second hydrogen atom is left in the vicinity of the Si-H bond formed by the first hydrogen atom. The high reactivity of atomic hydrogen causes formation of silyl and silylene functional groups. Beside observed changes in infrared absorption we can support our conclusion on aging of intercalated graphene by two-point resistance measurements. We have measured resistances in the range 1-70 kΩ for fresh QFSMLG samples and the resistance is increased up to 0.2-2 MΩ range within one to two weeks of air exposure. Although our experiments are not in agreement with literature[16,19] we believe that the contradiction is due to different experimental techniques used to probe stability of hydrogen intercalation. For example, the Low energy electron diffraction (LEED) was used in Ref. 19 to show unchanged LEED pattern after exposure to air for five days. We note, however, that no detailed analysis of diffraction spots' FWHM was performed. Contrary to LEED, the X-ray photo-electron spectroscopy (XPS) does show some degree of degradation, see Fig. S2 in supplementary information of Ref. 19. Therefore we conclude that the temporal stability of hydrogenated graphene is an issue which needs to be addressed.

IV. CONCLUSIONS

We have presented spectroscopic study of Si-H bond formation in hydrogen intercalated buffer layer and SLG on SiC. The Si-H bonds are well ordered at temperatures exceeding 1000°C, which is well above Si-H bond formation. Such elevated temperatures are needed to overcome additional barrier for hydrogen to get in the SiC/graphene interface through graphene lattice defects or to tunnel through the graphene and/or buffer layer lattice. The formation of QFSMLG and QFSBLG has been confirmed by Raman spectroscopy. We have also shown that the stability of hydrogen intercalated SLG is largely reduced due to the presence of highly reactive atomic hydrogen, which is left behind Si-H bond formation during decoupling of the buffer layer from SiC substrate. This reaction of atomic hydrogen tends to form silyl and silylene functional groups on the SiC/SLG surface, as shown by infrared absorption spectroscopy.

ACKNOWLEDGMENTS

Financial support from the Grant Agency of the Czech Republic under project 16-15763Y, and the project VaVpI CZ.1.05/4.1.00/16.0340 are gratefully acknowledged. We also acknowledge support of the Charles University Grant Agency under project GA UK No. 932216.

[1] B. Jouault, N. Camara, B. Jabakhanji, A. Caboni, C. Consejo, P. Godignon, D. K. Maude, and J. Camassel, "Quantum Hall effect in bottom-gated epitaxial graphene grown on the C-face of SiC," Appl. Phys. Lett. **100** (2012).
[2] T. Shen, J. J. Gu, M. Xu, Y. Q. Wu, M. L. Bolen, M. A. Capano, L. W. Engel, and P. D. Ye, "Observation of quantum-Hall effect in gated epitaxial graphene grown on SiC (0001)," Appl. Phys. Lett. **95** (2009).
[3] S. Tanabe, Y. Sekine, H. Kageshima, M. Nagase, and H. Hibino, "Half-integer quantum Hall effect in gate-controlled epitaxial graphene devices," Appl. Phys. Express **3** (2010).
[4] J. S. Moon, D. Curtis, S. Bui, M. Hu, D. K. Gaskill, J. L. Tedesco, P. Asbeck, G. G. Jernigan, B. L. VanMil, R. L. Myers-Ward, C. R. Eddy, Jr., P. M. Campbell, and X. Weng, "Top-gated epitaxial graphene FETs on Si-face SiC wafers with a peak transconductance of 600 mS/mm," IEEE Electron Device Lett. **31**, 260–262 (2010).
[5] D. Waldmann, J. Jobst, F. Speck, T. Seyller, M. Krieger, and H. B. Weber, "Bottom-gated epitaxial graphene," Nat. Mater. **10**, 357–360 (2011).
[6] D. Waldmann, J. Jobst, F. Fromm, F. Speck, T. Seyller, M. Krieger, and H. B. Weber, "Implanted bottom gate for epitaxial graphene on silicon carbide," Jour. Phys. D: Appl. Phys. **45** (2012).
[7] F. Fromm, P. Wehrfritz, M. Hundhausen, and Th. Seyller, "Looking behind the scenes: Raman spectroscopy of top-gated epitaxial graphene through the substrate," New J. Phys. **15** (2013).
[8] C. P. Puls, N. E. Staley, J.-S. Moon, J. A. Robinson, P. M. Campbell, J. L. Tedesco, R. L. Myers-Ward, C. R. Eddy, Jr., D. Kurt Gaskill, and Y. Liu, "Top-gate dielectric induced doping and scattering of charge carriers in epitaxial graphene," Appl. Phys. Lett. **99** (2011).
[9] K. Ullmann, P. B. Coto, S. Leitherer, A. Molina-Ontoria, N. Martin, M. Thoss, and H. B. Weber, "Single-molecule junctions with epitaxial graphene nanoelectrodes," Nano Lett. **15**, 3512–3518 (2015).
[10] K. V. Emtsev, F. Speck, Th. Seyller, L. Ley, and J. D. Riley, "Interaction, growth, and ordering of epitaxial graphene on SiC{0001} surfaces: A comparative photoelectron spectroscopy study," Phys. Rev. B **77** (2008).
[11] A. Mattausch and O. Pankratov, "Ab initio study of graphene on SiC," Phys. Rev. Lett. **99**, 076802 (2007).
[12] A. J. M. Giesbers, P. Prochazka, and C. F. J. Flipse, "Surface phonon scattering in epitaxial graphene on 6H-SiC," Phys. Rev. B **87** (2013).

[13] C. Yu, J. Li, Q. B. Liu, S. B. Dun, Z. Z. He, X. W. Zhang, S. J. Cai, and Z. H. Feng, "Buffer layer induced band gap and surface low energy optical phonon scattering in epitaxial graphene on SiC(0001)," Appl. Phys. Lett. **102** (2013).
[14] J. Lin, L. Guo, Y. Jia, R. Yang, S. Wu, J. Huang, Y. Guo, Z. Li, G. Zhang, and X. Chen, "Identification of dominant scattering mechanism in epitaxial graphene on SiC," Appl. Phys. Lett. **104** (2014).
[15] J. A. Robinson, M. Hollander, M. LaBella, K. A. Trumbull, R. Cavalero, and D. W. Snyder, "Epitaxial graphene transistors: Enhancing performance via hydrogen intercalation," Nano Lett. **11**, 3875–3880 (2011), pMID: 21805993.
[16] C. Riedl, C. Coletti, T. Iwasaki, A. A. Zakharov, and U. Starke, "Quasi-free-standing epitaxial graphene on SiC obtained by hydrogen intercalation," Phys. Rev. Lett. **103**, 246804 (2009).
[17] S. Forti, K. V. Emtsev, C. Coletti, A. A. Zakharov, C. Riedl, and U. Starke, "Large-area homogeneous quasifree standing epitaxial graphene on SiC(0001): Electronic and structural characterization," Phys. Rev. B **84** (2011).
[18] S. Watcharinyanon, C. Virojanadara, J. R. Osiecki, A. A. Zakharov, R. Yakimova, R. I. G. Uhrberg, and L. I. Johansson, "Hydrogen intercalation of graphene grown on 6H-SiC(0001)," Surf. Sci. **605**, 1662–1668 (2011).
[19] M. Amjadipour, A. Tadich, J. J. Boeckl, J. Lipton-Duffin, J. MacLeod, F. Iacopi, and N. Motta, "Quasi free-standing epitaxial graphene fabrication on 3C-SiC/Si(111)," Nanotechnology **29** (2018).
[20] C. Yu, Q. Liu, J. Li, W. Lu, Z. He, S. Cai, and Z. Feng, "Preparation and electrical transport properties of quasi free standing bilayer graphene on SiC (0001) substrate by H intercalation," Appl. Phys. Lett. **105**, 183105 (2014).
[21] J. Sforzini, L. Nemec, T. Denig, B. Stadtmueller, T. L. Lee, C. Kumpf, S. Soubatch, U. Starke, P. Rinke, V. Blum, F. C. Bocquet, and F. S. Tautz, "Approaching truly freestanding graphene: The structure of hydrogen-intercalated graphene on 6H-SiC(0001)," Phys. Rev. Lett. **114** (2015).
[22] K.-S. Kim, G.-H. Park, H. Fukidome, S. Takashi, K. Fumio, and M. Suemitsu, "A table-top formation of bilayer quasi-free-standing epitaxial-graphene on SiC(0001) by microwave annealing in air," arXiv:1705.06409 [cond-mat.mes-hall].
[23] J. Bao, W. Norimatsu, H. Iwata, K. Matsuda, T. Ito, and M. Kusunoki, "Synthesis of freestanding graphene on SiC by a rapid-cooling technique," Phys. Rev. Lett. **117** (2016).
[24] A. Stoehr, S. Forti, S. Link, A. A. Zakharov, K. Kern, U. Starke, and H. M. Benia, "Intercalation of graphene on SiC(0001) via ion implantation," Phys. Rev. B **94** (2016).
[25] P. Mondelli, B. Gupta, M. Grazia Betti, C. Mariani, J. Lipton Duffin, and N. Motta, "High quality epitaxial graphene by hydrogen-etching of 3C-SiC(111) thin-film on Si(111)," Nanotechnology **28** (2017).
[26] A. Sandin, J. E. (Jack) Rowe, and D. B. Dougherty, "Improved graphene growth in UHV: Pit-free surfaces by selective Si etching of SiC(0001)-Si with atomic hydrogen," Surf. Sci. **611**, 25–31 (2013).
[27] W. A. de Heer, C. Berger, M. Ruan, M. Sprinkle, X. Li, Y. Hu, B. Zhang, J. Hankinson, and E. Conrad, "Large area and structured epitaxial graphene produced by confinement controlled sublimation of silicon carbide," Proceedings of the National Academy of Sciences of the United States of America **108**, 16900–16905 (2011).
[28] J. Kunc, M. Rejhon, E. Belas, V. Dedic, P. Moravec, and J. Franc, "Effect of residual gas composition on epitaxial growth of graphene on SiC," Phys. Rev. Appl. **8** (2017).
[29] F. Speck, J. Jobst, F. Fromm, M. Ostler, D. Waldmann, M. Hundhausen, H. B. Weber, and Th. Seyller, "The quasi-free-standing nature of graphene on H-saturated SiC(0001)," Appl. Phys. Lett. **99**, 122106 (2011).
[30] M. S. Dresselhaus, A. Jorio, A. G. Souza Filho, and R. Saito, "Defect characterization in graphene and carbon nanotubes using Raman spectroscopy," Philos. Trans. Royal Soc. A **368**, 5355–5377 (2010).
[31] L. G. Cancado, K. Takai, T. Enoki, M. Endo, Y. A. Kim, H. Mizusaki, A. Jorio, L. N. Coelho, R. Magalhaes-Paniago, and M. A. Pimenta, "General equation for the determination of the crystallite size La of nanographite by Raman spectroscopy," Appl. Phys. Lett. **88** (2006).
[32] A. C. Ferrari and D. M. Basko, "Raman spectroscopy as a versatile tool for studying the properties of graphene," Nat. Nanotechnol. **8**, 235–246 (2013).
[33] J. A. Robinson, M. Wetherington, J. L. Tedesco, P. M. Campbell, X. Weng, J. Stitt, M. A. Fanton, E. Frantz, D. Snyder, B. L. VanMil, G. G. Jernigan, R. L. Myers-Ward, C. R. Eddy, Jr., and D. Kurt Gaskill, "Correlating Raman spectral signatures with carrier mobility in epitaxial graphene: A guide to achieving high mobility on the wafer scale," Nano Lett. **9**, 2873–2876 (2009).
[34] T. Masuda, A. Iwasaka, H. Takagishi, and T. Shimoda, "Polymeric precursor for solution-processed amorphous silicon carbide," J. Mater. Chem. C **3**, 12212–12219 (2015).
[35] M. Savoca, M. Andreas Robert George, J. Langer, and O. Dopfer, "Infrared spectrum of the disilane cation ($Si_2H_6^+$) from Ar-tagging spectroscopy," Phys. Chem. Chem. Phys. **15**, 2774–2781 (2013).
[36] W. R. Schmidt, L. V. Interrante, R. H. Doremus, T. K. Trout, P. S. Marchetti, and G. E. Maciel, "Pyrolysis chemistry of an organometallic precursor to silicon-carbide," Chem. Mater. **3**, 257–267 (1991).
[37] D. S. Xu, L. Sun, H. L. Li, L. Zhang, G. L. Guo, X. S. Zhao, and L. L. Gui, "Hydrolysis and silanization of the hydrosilicon surface of freshly prepared porous silicon by an amine catalytic reaction," New J. Chem. **27**, 300–306 (2003).
[38] Y. Kim and D. R. Olander, "Reaction of beta-SiC with thermal atomic-hydrogen by modulated molecular-beam mass-spectrometry," Surf. Sci. **313**, 399–416 (1994).